

Human herpesvirus 6 infection arrests cord blood mononuclear cells in G₂ phase of the cell cycle

Leen De Bolle^a, Sigrid Hatse^a, Erik Verbeken^b, Erik De Clercq^a, Lieve Naesens^{a,*}

^aRega Institute for Medical Research, Katholieke Universiteit Leuven, Minderbroedersstraat 10, B-3000 Leuven, Belgium

^bDepartment of Morphology and Molecular Pathology, Katholieke Universiteit Leuven, Minderbroedersstraat 12, B-3000 Leuven, Belgium

Received 5 December 2003; revised 5 January 2004; accepted 12 January 2004

First published online 28 January 2004

Edited by Hans-Dieter Klenk

Abstract We here report that after infection with human herpesvirus 6A, human cord blood mononuclear cells accumulate in G₂/M phase of the cell cycle. Experiments with foscarnet or ultraviolet (UV)-irradiated virus stocks pointed at an (immediate-)early, newly formed viral protein to be responsible for the arrest. At the molecular level, p53, cyclin B₁, cyclin A and tyrosine¹⁵-phosphorylated cdk1 accumulated after HHV-6A infection, indicating an arrest in G₂. However, no change was observed in the levels of downstream effectors of p53 in establishing a G₂ arrest, i.e. p21 and 14-3-3σ. We thus conclude that the HHV-6A-induced G₂ arrest occurs independently of p53 accumulation.

© 2004 Federation of European Biochemical Societies. Published by Elsevier B.V. All rights reserved.

Key words: Human herpesvirus 6; Cell cycle; Protein p53; Cyclin; Cyclin-dependent kinase

1. Introduction

HHV-6 (human herpesvirus 6) primary infection is the cause of exanthema subitum in young children [1]. This highly seroprevalent virus may reactivate during episodes of immune suppression (e.g. in transplant recipients or AIDS patients) causing disseminated infection of various organs [2]. Although HHV-6 has tentatively been linked to certain lymphoproliferative disorders, its oncogenic potential has not been established. Indeed, the ubiquitous nature of the pathogen, and its ability to remain in a latent state and to integrate into the host cell chromosomal DNA [3], complicate the interpretation of polymerase chain reaction (PCR) analysis on tumor tissue [4]. As a betaherpesvirus, HHV-6 (which exists as two variants, A and B) is closely related to HHV-7 and, more distantly, human cytomegalovirus (HCMV). HHV-6 has a broad in vivo cell tropism, but in vitro replication occurs most efficiently in T-lymphocytes and neural cells. Several effects of HHV-6 infection on host cell metabolism have

been described, such as modulation of the host cell's immune responses (reviewed in [5]), shutoff of cellular DNA synthesis [6] and stimulation of the host cell protein synthesis [7]. Moreover, HHV-6 is capable of inducing apoptosis both in continuous cell lines and in cord blood mononuclear cells (CBMCs) [8–10], and the protein encoded by the HHV-6 DR7 gene was shown to bind to p53 and to inhibit p53-activated transcription [11]. It was speculated by Braun et al. [12] that the virus might disrupt a component of the cell cycle that links cytoplasmic growth with cell division. The present report is the first detailed investigation into the effects of HHV-6 infection on cell cycling and underlying events.

2. Materials and methods

2.1. Cells and virus

Human CBMCs were isolated by density gradient centrifugation and cultured in RPMI medium supplemented with 10% fetal calf serum (FCS) (both from Life Technologies), 10 µg/ml phytohemagglutinin A and 10 U/ml interleukin-2 (IL-2) for 48 h (both from Roche). Cell-free virus preparations of HHV-6A (strain GS) and HHV-6B (strain Z29) were prepared as described before [13]. Titers were determined as viral DNA equivalents by quantitative PCR and confirmed by endpoint dilution of viral inocula on cell cultures. A multiplicity of infection of 10 virus particles per cell was used throughout our experiments. 24 h prior to infection, cells were transferred to a low-mitogen regimen (RPMI medium containing 10% FCS and 2 U/ml IL-2) at a density of 5×10^5 cells/ml.

2.2. Cell cycle analysis

Custom cell cycle analysis was performed on 10^6 cell nuclei at different time points post infection (p.i.) using the Cycle Test Plus DNA Reagent Kit (BD Biosciences) according to the manufacturer's instructions. Cell doublets were excluded from the fluorescence-activated cell sorter (FACS) analysis by conventional dot plot gating. Simultaneous staining of HHV-6 antigen and cellular DNA was performed as follows: 10^6 cells were fixed in 70% ethanol for 30 min at 4°C. After several washes with phosphate-buffered saline (PBS), cells were stained with a polyclonal antibody raised against the pU69 protein of HHV-6 [13] and subsequently with fluorescein isothiocyanate (FITC)-conjugated anti-rabbit IgG antibody (Dako). Cells were then treated with 0.1% Triton X-100 (Sigma), 20 µg/ml RNase A (Boehringer Mannheim) and stained with 10 µg/ml propidium iodide (Sigma) for 10 min, prior to FACS analysis.

2.3. Western blot analysis

Total protein from 2.5×10^6 CBMCs was extracted at different time points after HHV-6 infection and subjected to sodium dodecyl sulfate–polyacrylamide gel electrophoresis (SDS–PAGE) on 12% Tris–HCl gels (pH 8.8), electroblotting and antibody binding, as described previously [13]. Mouse monoclonal antibodies to cdk1, proliferating cell nuclear antigen (PCNA), p21^{waf1}, cyclin D1 and p53 (from Calbiochem), cdk2, cdc25C, cyclin B1, phospho-Tyr¹⁵-cdk1 and phospho-Ser²¹⁶-cdc25C (from Santa Cruz Biotechnology), and cyclins A and E (both from Pharmingen) were diluted to 0.1–0.5 µg/ml. The rabbit

*Corresponding author. Fax: (32)-16-337340.

E-mail addresses: leen.debolle@rega.kuleuven.ac.be (L. De Bolle), sigrid.hatse@rega.kuleuven.ac.be (S. Hatse), erik.verbeken@med.kuleuven.ac.be (E. Verbeken), erik.declercq@rega.kuleuven.ac.be (E. De Clercq), lieve.naesens@rega.kuleuven.ac.be (L. Naesens).

Abbreviations: CBMC, cord blood mononuclear cell; CPE, cytopathic effect; HCMV, human cytomegalovirus; HHV, human herpesvirus; HSV, herpes simplex virus; SDS–PAGE, sodium dodecyl sulfate–polyacrylamide gel electrophoresis; p.i., post infection

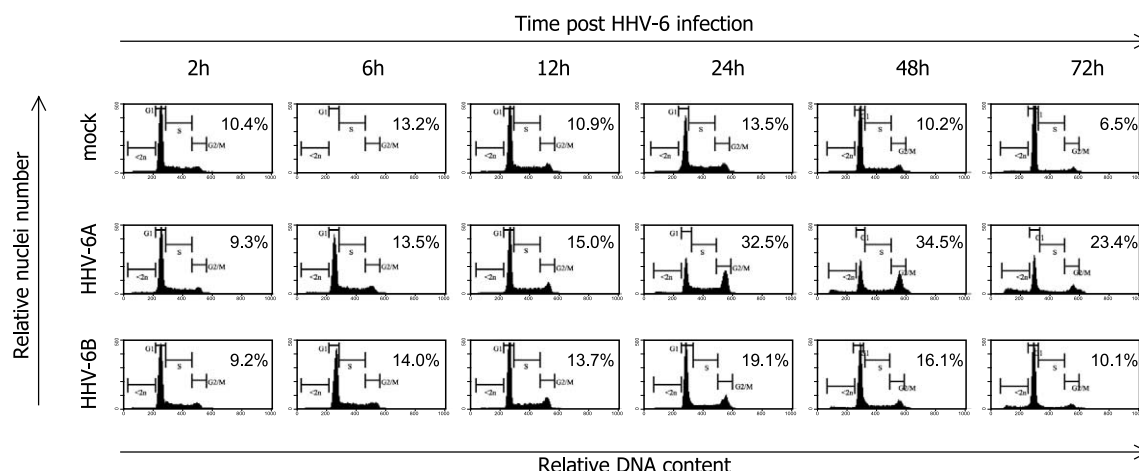


Fig. 1. HHV-6 infection induces G_2/M phase arrest. At different time points after infection of human CBMCs, the relative DNA content was determined by propidium iodide staining of cell nuclei and flow cytometric analysis. Numbers given are the mean percentages (from three experiments) of cells with a $4n$ DNA content. Debris and doublets were excluded from the analysis by conventional dot plot gating. Histograms shown are from one experiment, representative of three independent experiments.

polyclonal antisera raised against the HHV-6 proteins pU90 (kind gift of Dr. Y. Inoue) and pU69 [13] were diluted 1/500. Detection of the horseradish peroxidase-labeled immune complexes was performed using the chemiluminescence ECL Plus detection system (Amersham).

2.4. Immunofluorescence analysis

Aliquots of 5×10^4 cells were spotted onto glass slides and allowed to dry prior to fixation in ice-cold methanol for 5 min. For FACS analysis, 5×10^5 cells were washed with PBS and fixed with 4% formaldehyde for 10 min at 4°C . Simultaneous detection of viral and cellular proteins was carried out by overnight incubation at 4°C with primary antibody from different species. Secondary FITC- and tetra-rhodamine isothiocyanate (TRITC)-labeled antibodies were added for 45 min at 37°C . Antibodies were diluted in PBS containing 1% FCS and 0.1% Tween 20. Slide preparations were finally mounted in Vectashield medium (Vector Laboratories). Samples for flow cytometry were fixed in 1% formaldehyde in PBS and analyzed on a FACScan flow cytometer (BD Biosciences). As a negative control for non-specific background staining, cells were stained in parallel with secondary antibody alone.

3. Results and discussion

3.1. Interference of HHV-6 with cell cycle progression

To investigate the influence of HHV-6 infection on cell cycle progression, we investigated the DNA content of CBMCs after infection with HHV-6 at high multiplicity of infection (MOI) (10 viral particles per cell). Similar to the observation made by Secchiero et al. for HHV-7 [14], a marked accumulation of cells in G_2/M phase of the cell cycle was observed in HHV-6-infected vs. mock-infected cells from 12 h p.i. onwards (Fig. 1). This effect increased over time up to 48 h p.i. (cell viability at later time points declined due to cytopathic effects (CPEs)) and was most pronounced after HHV-6A infection (34.5% cells in G_2/M phase vs. 10.2% in the mock-infected condition). The proportion of cells in S phase remained constant at about 20% of the population until 72 h p.i., when it dropped to 8% in the mock-infected conditions, but remained unchanged in infected conditions. When DNA content and HHV-6 pU69 antigen expression were determined simultaneously by FACS analysis, pU69-positive cells appeared in both the $2n$ and $4n$ populations (Fig. 4, upper panel). Nevertheless, the distribution of pU69-positive cells was more pronounced towards G_2/M arrest (55% vs. 34%

for the whole population of HHV-6-infected cells). In parallel with cell cycle analysis, cell numbers were determined; mock-infected cells had doubled by 48 h p.i. and undergone two rounds of replication after 96 h, whereas in HHV-6A-infected cells no increase in cell number was observed over time, strong CPE was visible as from 48 h p.i. and cell viability was 50% after 72 h. Cells infected with HHV-6B showed an intermediate growth pattern and minor CPE (data not shown). The viral immediate-early pU90 and early pU69 antigens were quantified by Western blot (Fig. 3) to ensure that equal multiplicities of infection were used for both A and B variants. However, since differences in replication efficiency

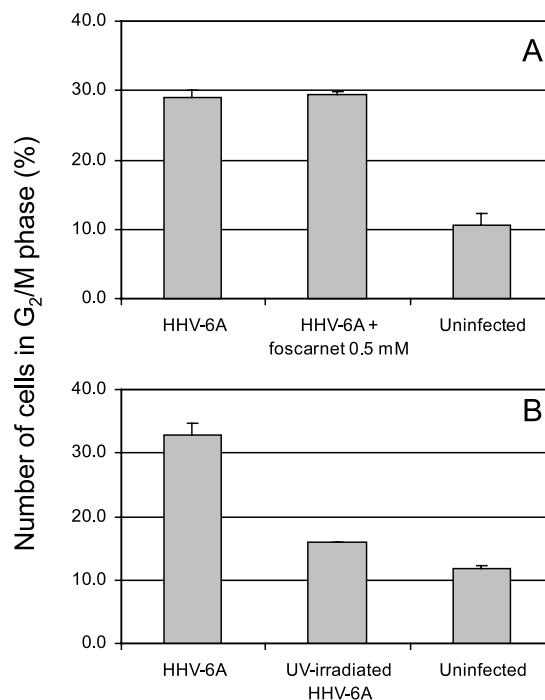


Fig. 2. Effect of foscarnet (0.5 mM) (A) and UV irradiation (B) on the HHV-6A-induced G_2/M arrest at 48 h p.i. Data shown are the results (\pm S.D.) from two independent experiments, each performed in duplicate.

between both variants have been described according to the cell type used [15], and our HHV-6A and HHV-6B virus stocks were passaged on different cell lines, the observed differences in the cell cycle effects of the A and B variants may be difficult to interpret.

To further characterize the observed effect of HHV-6A infection on the cell cycle, mock- and HHV-6A-infected CBMCs were treated with 0.5 mM foscarnet upon infection and cell cycle analysis was performed at 48 h (Fig. 2A), 72 h and 96 h p.i. (not shown). No differences in cell cycle distribution were observed between foscarnet-treated and untreated cells, neither in mock- nor in HHV-6A-infected conditions. In spite of the inhibition of viral replication by foscarnet (as ascertained by the absence of viral DNA and protein at 96 h p.i. (data not shown)), the foscarnet-treated HHV-6A-infected cells accumulated in G₂/M. This points at an immediate-early or early event in the viral replication cycle to be responsible for the cell cycle arrest, as late protein synthesis is virtually abolished by high-dose foscarnet. In order to determine whether the HHV-6-induced G₂/M arrest requires virus replication, the HHV-6A stock was ultraviolet (UV)-irradiated for 20 min. This treatment reduced virus infectivity by >95% as determined by infection of Sup-T1 lymphoblastoma cells and quantitation of viral protein at 4 days p.i. (data not shown). UV irradiation eliminated the virus' capacity of inducing a G₂/M arrest (Fig. 2B), indicating that de novo viral protein synthesis is a prerequisite for the virus-induced cell cycle arrest to occur. Events at the level of HHV-6 binding and entry, or proteins present in the tegument of the virus particle apparently do not exert important effects here – in contrast to the HCMV-induced arrest at the G₁/S boundary in which the tegument proteins pUL69 and pp71 actively participate [16]. Mitogenic stimulation of CBMCs is a prerequisite for their infection by HHV-6 [17]. However, to investigate

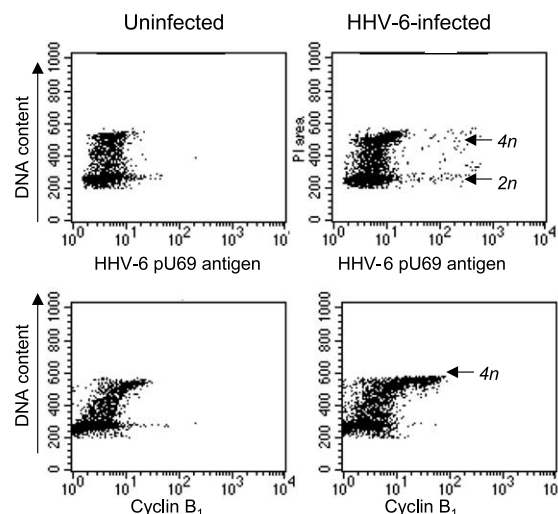


Fig. 4. Scatter plot analysis of uninfected (left) and HHV-6-infected (right) CBMCs at 48 h p.i. Cells were stained simultaneously for HHV-6 pU69 antigen (upper panel) or cyclin B₁ (lower panel) expression and for DNA content as described in Section 2. Cells showing high antigen expression are marked by arrows.

whether HHV-6, like HCMV, can force cells to enter the cell cycle (i.e. pass the G₀/G₁ transition) prior to arresting them, we performed an experiment in which no mitogens were added to freshly isolated CBMCs, and HHV-6A was added immediately upon isolation. Cell cycle analysis, performed as described above at 6 h intervals between 0 and 30 h p.i., revealed that >95% of both the mock-infected and HHV-6A-infected cell populations had a DNA content corresponding to the G₁ (or G₀) phase and, hence, no measurable induction of the cell cycle was observed (data not shown).

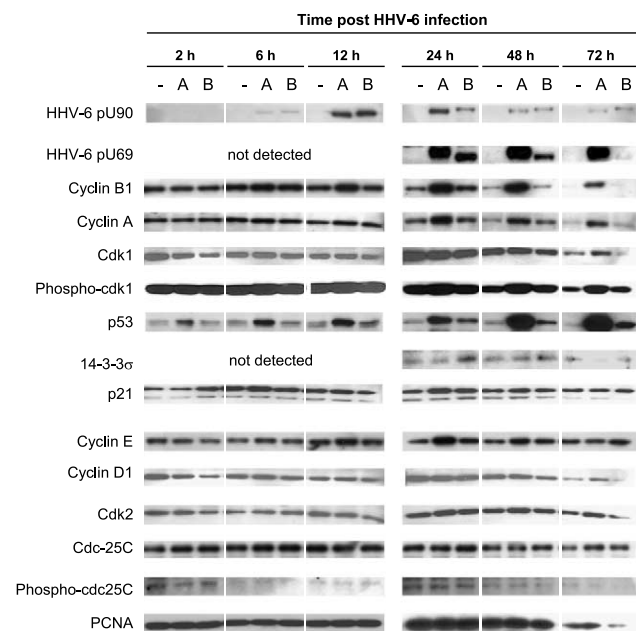


Fig. 3. Western blot analysis of steady-state levels of a panel of proteins involved in cell cycle control. Human CBMCs were infected with HHV-6A (A) or HHV-6B (B) or mock infected (–). At different time points after infection, protein extracts were prepared and 10 µg of total protein was analyzed by SDS-PAGE, electroblotting and enhanced chemiluminescence detection.

3.2. Effect of HHV-6 infection on selected cell cycle protein expression levels

In order to characterize the underlying molecular events involved in the described G₂/M arrest, the steady-state protein levels of several key players in cell cycle regulation were determined by Western blotting (Fig. 3). A manifest accumulation of cyclins A and B₁, involved in S phase and G₂/M transition, was observed in HHV-6A-infected conditions from 12–24 h p.i. onwards. The fact that cyclin B₁, although clearly upregulated in the HHV-6A-infected condition, does not localize to the same cells as HHV-6 pU69 (Fig. 5, panel 2), does not exclude a role for HHV-6 in cyclin B₁ accumulation, as pU69 most likely is not involved and may show a different temporal expression pattern. Moreover, the cytoplasmic localization of cyclin B₁ after HHV-6A infection suggests a G₂ arrest, rather than an arrest in mitosis, when cyclin B₁ is present in the nucleus. A less pronounced accumulation of cyclin B steady-state levels was also reported after HHV-7 infection (albeit at later time points) [14]. However, whereas after HHV-7 infection, cyclin B expression was reported to be unscheduled, cyclin B₁ upregulation after HHV-6A infection was confined to cells with a DNA content of 4n (Fig. 4, lower panel). Neither did we observe an accumulation of total cdk1 (as reported for HHV-7), although a significant increase of its Tyr¹⁵-phosphorylated form became apparent from 24 h p.i. onwards, in parallel with cyclin B₁ levels. This agrees entirely

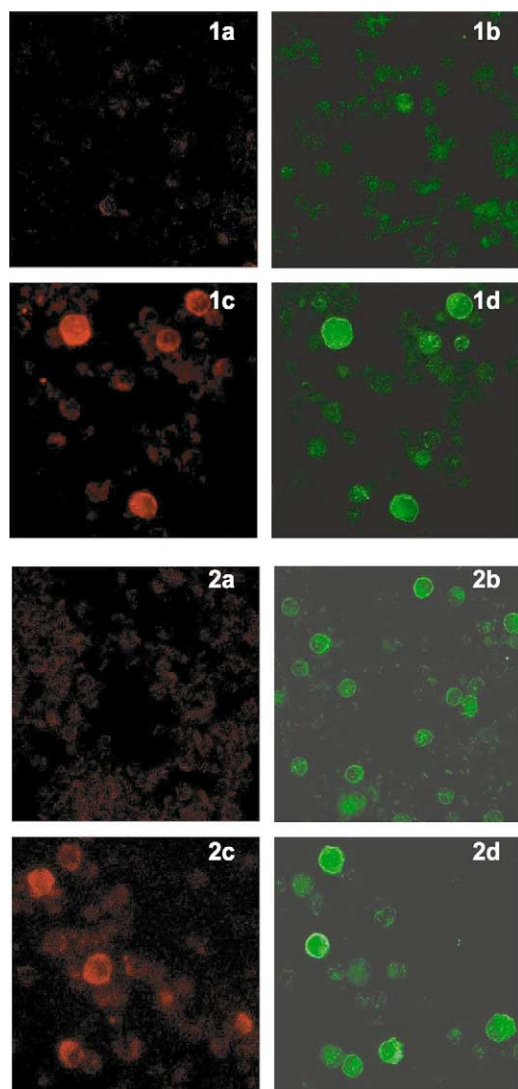


Fig. 5. Expression patterns of p53 and cyclin B₁ in uninfected (a and b) and HHV-6-infected (c and d) CBMCs at 48 h p.i. The same field of cells was stained simultaneously for the HHV-6 pU69 antigen (red fluorescence) and either p53 (panel 1) or cyclin B₁ (panel 2), both visualized as green fluorescence. Original magnification: 400 \times .

with our data on the altered cell cycle distribution after HHV-6A infection, and points to a maintained G₂ arrest, as dephosphorylation of the tyrosine residue at position 15 of cdk1 is a prerequisite for entry into mitosis [18]. Cyclin E, which peaks at G₁/S transition, was slightly augmented at 24 h p.i. in the HHV-6A-infected condition, but this effect was not maintained at later time points. These findings contrast with the HCMV-induced G₂/M arrest in cycling cells, where induction of high levels of cyclin E was reported and cyclin A appeared only at late time points [19].

We observed no HHV-6-induced alterations in the steady-state levels of cyclin D₁ (the G₁-specific cyclin) and cdk2, although it should be noted that protein expression levels do not necessarily correlate with activity levels. Furthermore, HHV-6 infection did not alter the expression of PCNA and of cdc25C – both the total cdc25C protein and its Ser²¹⁶-phosphorylated form, which occurs after Chk-1/2-induced phosphorylation in response to e.g. DNA damage [18]. Both

PCNA and cdc25C are involved in the G₂/M checkpoint through specific interactions with each other, p21 and the cdk1/cyclin B complex [20,21].

The protein most manifestly affected by HHV-6A infection was the tumor suppressor protein p53, an important effector molecule that acts in multiple ways: it is capable of inducing a cell cycle arrest both in G₁ phase and at the entry into mitosis (DNA damage checkpoint) [18]. On the other hand, p53 is capable of inducing apoptosis if cellular DNA is damaged beyond repair [22]. A strong accumulation of p53 has also been observed following expression of the herpes simplex virus (HSV)-1 ICP0 protein [23] and after HCMV [19,24,25] infection. Moreover, the protein encoded by the HHV-6 immediate-early DR7 gene (pDR7) was shown to bind and stabilize p53, and to repress its transcriptional activities [11]. Our observations support this finding. Indeed, the accumulation of p53 after HHV-6 infection was the earliest detectable event, initiating as soon as 2 h p.i. (Fig. 3). Moreover, p53-positive cells are strongly positive for HHV-6A pU69 (Fig. 5, panel 1). However, if the accumulation of p53 would correlate with an enhanced activity, one would expect p21 and 14-3-3 σ to be induced and cdk1 and cyclin B₁ levels to decline – since their transcription is regulated by p53 [18]. This was clearly not the case in our experiments. One could thus assume that the accumulated p53 is inactive as a transcription factor, e.g. through binding of pDR7 or through alteration of its cellular distribution, since active p53 is located in the nucleus [26]. In HHV-6A-infected cells, p53 seems present in the cytoplasm (Fig. 5, panel 1d). A similar observation was made after HCMV infection [27,28], although sequestration of p53 in viral replication centers in the nucleus has also been reported [29]. On the other hand, the observed p53 induction correlates with the emerging apoptotic fraction (cells with a hypodiploid DNA content) in HHV-6A- and HHV-6B-infected conditions from 24 h p.i. onwards (Fig. 1). Whereas the hypodiploid fraction in mock-infected CBMCs remained below 2%, it increased to 3.6, 10.9 and 21.7% after HHV-6A infection at 24, 48 and 72 h, respectively. Apoptosis, the second major outcome of p53 induction, may occur independently of the transcriptional activities of p53 [22] and has been reported to be induced by HHV-6 infection, although the underlying mechanisms are not yet fully understood [8–10]. In summary, based on the observations that steady-state levels of p21, 14-3-3 σ and Ser²¹⁶-phosphorylated cdc25C remain unaffected after HHV-6A infection, whereas cyclin B₁, Tyr¹⁵-cdc2 and p53 accumulate, we conclude that mechanisms other than p53 or Chk-1 activation, and possibly implying virally encoded factors, may be responsible for the observed G₂ arrest.

3.3. Conclusion

The data presented here show that the cell cycle distribution shifts towards cells with a 4n DNA content after HHV-6A infection of CBMCs, as has been described for HHV-7-infected CD4⁺ T-lymphocytes and Sup-T1 cells [14]. It remains to be demonstrated, however, whether the underlying effectors (other than cyclin B) are affected in a similar way by these two viruses. The effects of HHV-6 (and HHV-7) on cell cycling are quite different from those observed for the other herpesviruses, HSV-1 and HCMV, which can arrest the cell cycle at multiple stages. In the case of HCMV infection, divergent effects were observed depending on the cell's permissiveness and synchronization status, and different viral proteins were

found to exert opposite effects on cell cycling [16]. The main outcome for both HSV-1 and HCMV is an arrest at the G₁/S transition, which is considered the optimal environment for viral replication without competition with the cellular DNA replication machinery. We found no evidence for HHV-6 to induce such an arrest. Moreover, although HCMV has been described to arrest cells in G₂/M phase in well-defined conditions, the underlying molecular expression patterns are clearly different from those observed for HHV-6A. This may explain our observation that the cdk inhibitor roscovitine, which is active against HSV-1 and HCMV [30], has no activity against HHV-6 (L. De Bolle, unpublished data).

In conclusion, our data on the G₂/M arrest induced by HHV-6A warrant further investigation into the underlying molecular events responsible for the altered expression of certain key players in the G₂/M transition. This, together with the identification of the individual HHV-6 proteins responsible for this cell cycle arrest, will increase our insight into the CPEs of this herpesvirus.

Acknowledgements: The authors wish to thank Kristien Minner for excellent technical assistance. L.D.B. and S.H. are Research Assistant and postdoctoral Research Assistant, respectively, of the 'Fonds voor Wetenschappelijk Onderzoek (FWO) – Vlaanderen'. This work was supported by grants from the FWO (no. G.0104.98) and the Belgian (Flemish Community) 'Geconcerteerde Onderzoeksacties' (GOA, no. 2000/12).

References

- [1] Yamanishi, K., Okuno, T., Shiraki, K., Takahashi, M., Kondo, T., Asano, Y. and Kurata, T. (1988) *Lancet* 1, 1065–1067.
- [2] Ljungman, P. (2002) *J. Infect. Dis.* 186 (Suppl. 1), S99–S109.
- [3] Morris, C., Luppi, M., McDonald, M., Barozzi, P. and Torelli, G. (1999) *J. Med. Virol.* 58, 69–75.
- [4] Daibata, M., Taguchi, T., Nemoto, Y., Taguchi, H. and Miyoshi, I. (1999) *Blood* 94, 1545–1549.
- [5] Dockrell, D.H. (2003) *J. Med. Microbiol.* 52, 5–18.
- [6] Di Luca, D., Katsafanas, G., Schirmer, E.C., Balachandran, N. and Frenkel, N. (1990) *Virology* 175, 199–210.
- [7] Black, J.B., Lopez, C. and Pellett, P.E. (1992) *Virus Res.* 22, 13–23.
- [8] Ichimi, R., Jin-no, T. and Ito, M. (1999) *J. Med. Virol.* 58, 63–68.
- [9] Yasukawa, M., Inoue, Y., Ohminami, H., Terada, K. and Fujita, S. (1998) *J. Gen. Virol.* 79, 143–147.
- [10] Inoue, Y., Yasukawa, M. and Fujita, S. (1997) *J. Virol.* 71, 3751–3759.
- [11] Kashanchi, F., Araujo, J., Doniger, J., Muralidhar, S., Hoch, R., Khleif, S., Mendelson, E., Thompson, J., Azumi, N., Brady, J.N., Luppi, M., Torelli, G. and Rosenthal, L.J. (1997) *Oncogene* 14, 359–367.
- [12] Braun, D.K., Dominguez, G. and Pellett, P.E. (1997) *Clin. Microbiol. Rev.* 10, 521–567.
- [13] De Bolle, L., Michel, D., Mertens, T., Manichanh, C., Agut, H., De Clercq, E. and Naesens, L. (2002) *Mol. Pharmacol.* 62, 714–721.
- [14] Secchiero, P., Bertolaso, L., Casareto, L., Gibellini, D., Vitale, M., Bemis, K., Aleotti, A., Capitani, S., Franchini, G., Gallo, R.C. and Zauli, G. (1998) *Blood* 92, 1685–1696.
- [15] Ablashi, D.V., Balachandran, N., Josephs, S.F., Hung, C.L., Krueger, G.R., Kramarsky, B., Salahuddin, S.Z. and Gallo, R.C. (1991) *Virology* 184, 545–552.
- [16] Kalejta, R.F. and Shenk, T. (2002) *Front Biosci.* 7, d295–d306.
- [17] Frenkel, N., Roffman, E., Schirmer, E.C., Katsafanas, G., Wyatt, L.S. and June, C.H. (1990) *Adv. Exp. Med. Biol.* 278, 1–8.
- [18] Taylor, W.R. and Stark, G.R. (2001) *Oncogene* 20, 1803–1815.
- [19] Jault, F.M., Jault, J.M., Ruchti, F., Fortunato, E.A., Clark, C., Corbeil, J., Richman, D.D. and Spector, D.H. (1995) *J. Virol.* 69, 6697–6704.
- [20] Ando, T., Kawabe, T., Ohara, H., Ducommun, B., Itoh, M. and Okamoto, T. (2001) *J. Biol. Chem.* 276, 42971–42977.
- [21] Kawabe, T., Suganuma, M., Ando, T., Kimura, M., Hori, H. and Okamoto, T. (2002) *Oncogene* 21, 1717–1726.
- [22] Vousden, K.H. and Lu, X. (2002) *Nat. Rev. Cancer* 2, 594–604.
- [23] Hobbs, W.E. and DeLuca, N.A. (1999) *J. Virol.* 73, 8245–8255.
- [24] Muganda, P., Mendoza, O., Hernandez, J. and Qian, Q. (1994) *J. Virol.* 68, 8028–8034.
- [25] Speir, E., Modali, R., Huang, E.S., Leon, M.B., Shawl, F., Finkel, T. and Epstein, S.E. (1994) *Science* 265, 391–394.
- [26] Ryan, K.M., Phillips, A.C. and Vousden, K.H. (2001) *Curr. Opin. Cell Biol.* 13, 332–337.
- [27] Wang, J., Belcher, J.D., Marker, P.H., Wilcken, D.E., Vercellotti, G.M. and Wang, X.L. (2001) *J. Mol. Med.* 78, 642–647.
- [28] Kovacs, A., Weber, M.L., Burns, L.J., Jacob, H.S. and Vercellotti, G.M. (1996) *Am. J. Pathol.* 149, 1531–1539.
- [29] Fortunato, E.A. and Spector, D.H. (1998) *J. Virol.* 72, 2033–2039.
- [30] Schang, L.M. (2002) *J. Antimicrob. Chemother.* 50, 779–792.